i-ETC: ISEL Academic Journal of Electronics, Telecommunications and Computers
CETC2016 Issue, Vol. 3, n. 1 (2017) ID-8

Benchtop SS-OCT – layout and performance evaluation

José P. Domingues[a,b], Susana F. Silva[b], Rui Bernardes[b] and A.M. Morgado[a,b]
[a] Department of Physics, University of Coimbra, Coimbra, Portugal
[b]IBILI, Faculty of Medicine, University of Coimbra, Coimbra, Portugal
jpd@uc.pt susana.f.s.89@gmail.com rmbernardes@fmed.uc.pt miguel@fis.uc.pt

Abstract — **Optical coherence tomography (OCT) is a non-invasive biomedical imaging technique that provides high speed and high resolution three dimensional and cross sectional images of biological samples, *in vivo* and *in situ*. OCT applications targeting small animals is believed to bring developments in medical techniques, instruments, diagnosis and therapies for a number of human diseases as always have been the case of animal experimentation.**

With the swept source OCT (SS-OCT) system presented in this work, we were able to achieve performance parameters that meet the requirements to image the retina of small animals. Performance characteristics include 105 dB for system sensitivity, a roll-off below 1 dB/mm over 3 mm depth and an axial resolution of 8 µm. We describe the layout and acquisition/processing solutions towards fast imaging of *in vivo* samples.

Keywords— **Swept Source OCT, Imaging, Instrumentation.**

I. Introduction

Since its first appearance in the early 1990's, Optical Coherence Tomography (OCT) was recognized as a very helpful tool for ophthalmology. Based on the optical interference phenomenon, the OCT is capable of producing high-resolution cross-sectional images of non-homogeneous samples, among which the biological tissue, being particularly tailored to image ocular structures such as the retina. Over the last twenty years, OCT has experienced a fast and steady growth. It now offers a wide range of applications, is clinically very well accepted and is the subject of active research worldwide. The technique and theory behind it – in all possible configurations, being it Time-Domain OCT (TD-OCT), Spectral-Domain OCT (SD-OCT) or Swept-Source OCT (SS-OCT) – is extensively described in the literature [1][2][3][4].

SS-OCT has been appointed as the most promising technology for OCT imaging by offering higher scanning speed, reduced sensitivity roll-off and better overall performance, when associated with balanced detection,[3] in comparison to time and Fourier/spectral domain approaches. OCT systems specifically developed to image small animals, used as physiological models of disease, are fundamental to test and develop new medical therapies. Our group is engaged in the development of a dedicated SS-OCT platform for small animals based on the most recent technological advances. It should allow testing different configurations and explore new concepts. The basic layout has already been presented [5] along with simulations and preliminary performance evaluation. In this paper, we report recent developments regarding *in vitro* performance and discuss key details with respect to acquisition/scanning synchronism.

The motivation for this development is definitely the possibility of building a valuable tool for research using animal models of disease.

In the field of biomedical research, small animals are very often used to develop, validate and test new techniques and therapies. OCT imaging can provide researchers with the means to understand physiology, pathology and phenotypes in health and disease.

Furthermore, this benchtop OCT system can be used as a platform for the continuing development and test of new OCT components, instrumentation and methods.

II. Materials and Methods

In its simpler formulation, the OCT can be considered as an open-air Michelson interferometer (Fig 1) with a beam-splitter, reference and sample paths and a Gaussian-shaped broadband source.

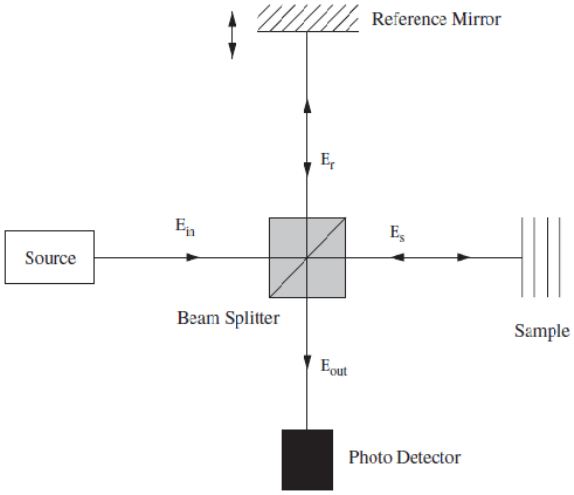

Fig. 1 Michelson interferometer schematics based OCT.

Light coming from the source can be represented by its electric field wave component E_{in} expressed as a complex exponential [1][2]:

$$E_{in} = s(w)e^{i(wt-kz)} \quad (1)$$

where s(w) is the source amplitude spectrum, w the angular frequency, k the wavenumber and z the distance along the propagation direction. Phase appears due to different interactions throughout the interferometer both for the reference and the sample arms, respectively:

$$E_R = (T_r T_s)^{1/2} E_{in} e^{-i2knz_R} \quad (2)$$

$$E_S = (T_r T_s)^{1/2} E_{in} e^{-i2knz_S} \quad (3)$$

where n is the refraction index, z_R and z_S are the path lengths in the reference and sample arms and the factor of 2 arises from the double pass of light. T_r and T_s are the beam-splitter reference and sample arm intensity transmission coefficients. The sample is not a simple reflecting surface and has a multilayered structure with each layer interface having a reflectance, r, given by the Fresnel's equations.

The internal sample refraction index structure is revealed by the E_{out} field that results from superposition (interference) of E_S and E_R.

Optical detectors measure Irradiance, which is proportional to the square of the amplitude of the E field. The detector output photocurrent, I(w,k), is proportional to the time average of the Irradiance and can be written as:

$$I(w,k) = \lim_{T\to\infty} \frac{1}{2T} \rho \int_{-T}^{T} E_{out} E_{out}^{*}\, dt \quad (4)$$

where ρ represents detector responsivity. Photocurrent appears as a sum of a self-interference term (arising from source self-interference and autocorrelation from the multiple reflectors of the sample) and a cross-interference term.

$$I(k) = I_0 + \rho S(k) \sqrt{R_r R_{S_n}} cos2k\left(z_r - z_{S_n}\right) \quad (5)$$

I_0, also called the dc term, accounts for all self-interference contributions. The second term, obtained by using the Euler's formula, is the cross-interference term, which contains the information on the sample structure. R is the power reflectance and subscripts S_n and r refer to sample layer n and reference mirror respectively.

Following Time-domain OCT, the technique evolved to the Fourier-domain OCT where the interference information is spatially encoded (SD-OCT), requiring a detector array, or time encoded (SS-OCT). In this case, a single-element detector is enough but the broadband source must be wavelength-swept and the data acquisition system must handle high acquisition rates. In the Fourier domain, the reference plan is fixed, an important advantage over Time-domain OCT, which requires mechanical sweeping of the reference mirror position. The layout presented here corresponds to fiber optic based SS-OCT.

III. Experimental Apparatus

A. OCT layout

The basic SS-OCT layout, composed of interferometer, scanning and acquisition system, is schematically depicted in Fig 2. The fundamental blocks of the system are: an Axsun Laser Swept-Source AXP50125-3 1060 nm (Axsun Technologies, Billerica, MA, USA), with central 1060 nm wavelength, 110 nm bandwidth and sweep frequency of 100 kHz; a 400 MSPS multi I/O acquisition board (X5-400M – Innovative Integration, California, USA) with two A/D and two D/A channels; an InGaAs balanced amplified photodetector (PDB471C – Thorlabs) and a X-Y positioning/scanning system (GSV002 Galvo Scanning System, Thorlabs GmbH, Germany). Optical components such as fiber cables, attenuators, couplers, polarization controllers, collimators and focusing objectives complete the system.

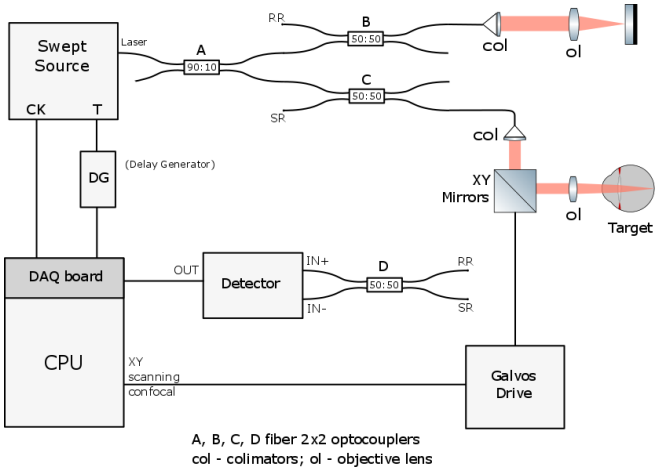

Fig. 2 – Overall SS-OCT Layout

The scanning, for cross-sectional (B-scan) and volume scans, is ensured by a X and Y galvanometer/mirror system which is controlled, respectively, through a precision waveform generator (AFG3101 Arbitrary Function Generator, Tektronix) and a DAC board (NI 6010, National Instruments, Austin, Texas). Digitized fringe data undergoes Fourier analysis to produce individual A-scans (along the beam direction), which can be composed in final B-scan images (XZ) and/or volumes (XYZ). These tasks are carried out by dedicated acquisition/control and processing software. Configuration parameters in the software can be tuned according to the needs: the scanning angles, the number of A-scans per B-scan and number of B-scans per volume. After acquisition, the whole volume can be stored for posterior analysis or discarded.

Overall timing parameters that determine the A-scan rate, A/D conversion sampling time and scanning positioning are obtained from two output signals provided by the laser source: SWEEP TRIGGER and K-CLOCK. Fig 3 shows the characteristics of the trigger and clock signals as well as the optical power at the useful sweep range.

B. Software

A customizable software was developed using object-oriented programming (Microsoft Visual C++/IDE) for the 64-bit Microsoft Windows 7 operating system resorting to libraries from Innovative Technologies to deal with data acquisition and hardware control.

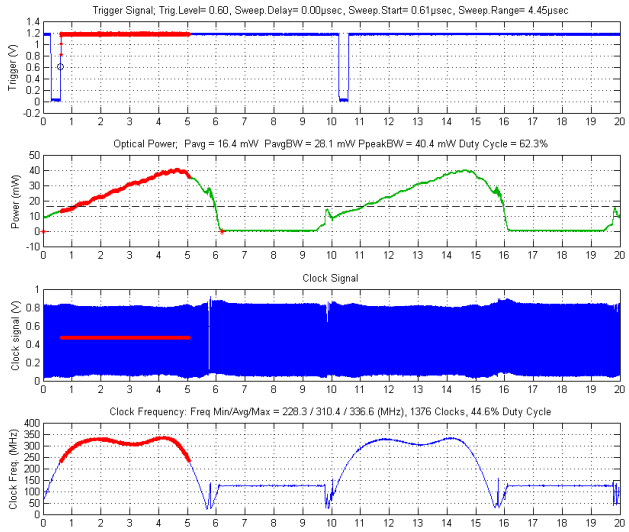

Fig. 3 – Typical spectral power, trigger and clock data for the Axsun source (from Axsun OCT source manual Rev. 09)

With the current hardware implementation, 1510 data points are digitalized in less than 5 µs, which correspond to the number of sample wavelengths outputted by the laser source. A full frequency sweep corresponds to the entire A-scan that can be computed owing to the Fourier transform. The number of useful data points is, nevertheless, restricted to 1376, with the remaining ones produced by the dummy clock outputted by the laser source.

TABLE 1

TYPICAL SCAN PARAMETERS (FROM AXSUN OCT SOURCE MANUAL REV. 09)

Parameter	**Value**
Wavelength Range	985.0-1095.0 nm
Sweep Frequency	100 kHz
Maximum Samples	1510
Selected Number of Samples	1376
Duty Cycle	45%

Synchronization between the acquisition and laser emission is paramount for SS-OCT. As such, the laser source has an embedded Mach-Zehnder interferometer (MZI) to provide an uniform clock signal in the wavenumber space (k-space). This allows direct A/D sampling of the optical detector signal event though the wavelength sweep of the laser output is non-linear. The period of the k-clock signal is defined by the free spectral range of MZI. Linearized fringe signals with equal k-spacing can be achieved by clocking the high-speed A/D channel of the acquisition board with the clock provided by the source. The Fourier transform analysis can then be directly applied to the acquired data. Moreover, the laser source also provides a trigger signal which is connected to the SYNC port of the acquisition board. This signal is responsible for starting the I/O module. Fig 4 shows a typical result of an A-Scan obtained over a 1 mm thickness glass.

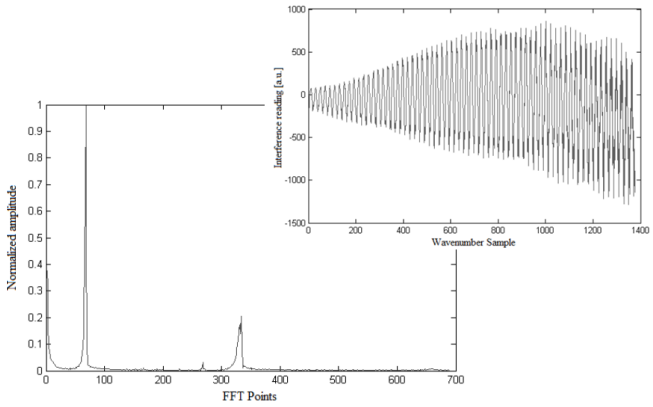

Fig. 4 - Interferogram and FFT spectrum for 1mm thick coverglass. Peaks represent air-glass and glass-air interfaces.

IV. PERFORMANCE ANALYSIS

The performance of the system was established based on commonly parameters found on the literature [6][7]: axial resolution (AR), sensitivity (S), dynamic range (DR) and depth sensitivity roll-off. Preliminary results have been obtained with current setup which compares and surpass the required values for biomedical applications which are listed in table 2.

TABLE 2

MINIMUM VALUES FOR THE MAIN OCT PARAMETERS IN BIOMEDICAL APPLICATIONS.[6] [7]

Parameter	**Value**
Axial Resolution	$< 10\ \mu m$
Sensitivity Fall-Off	$20\ dB$ over $2\ mm$ depth
Dynamic Range	$40 - 50\ dB$
Sensitivity	$> 95 dB$

The Point Spread Function (PSF), the system's response to a point object (or impulse), corresponds, for the described OCT system, to the Fourier transform of the interference signal due to a single, perfect reflector. This is accomplished using a gold mirror as sample. The PSF of the OCT system is shown in Fig 5.

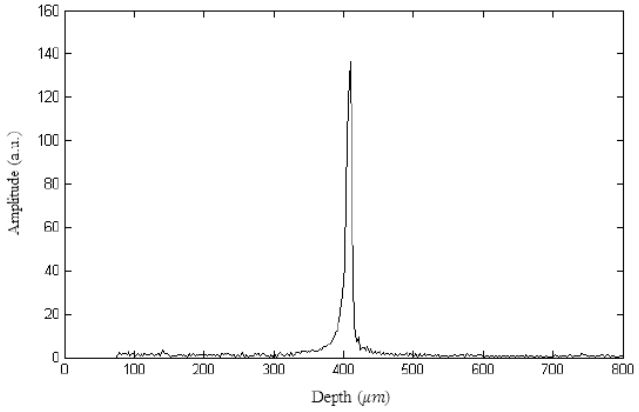

Fig. 5 – Point Spread Function using a gold mirror reflector

A. Axial Resolution

Axial or depth resolution is one of the key parameters to evaluate an OCT system performance. It is defined as the shortest interface separation that can be measured along the light beam´s propagation direction. The theoretical value of the axial resolution, usually specified in the air and assuming a Gaussian laser beam power spectrum, can be calculated as follows. Being

$$S(k) = \frac{1}{\sigma_k\sqrt{2\pi}} \exp\left[-\frac{(k-k_0)^2}{2\sigma_k^2}\right] \quad (6)$$

the Gaussian power spectrum and

$$\Delta k = (2\sqrt{2\ln(2)})\sigma_k \quad (7)$$

its full width at half maximum (FWHM), its Fourier transform is given by

$$\gamma(z) = \frac{1}{\sqrt{\pi}} \exp\left[-\frac{\Delta k^2 (z-z_0)^2}{16\ln(2)}\right] \quad (8)$$

This is the coherence function whose FWHM corresponds to the coherence length of the laser beam. If we used the well established criterium of defining the axial resolution as half of the source coherence length, we obtain for our system (λ_0=1060 nm and $\Delta\lambda$=100 nm).

$$z - z_0 = \Delta z = \frac{2ln(2)\lambda_0^2}{\pi\Delta\lambda} = 4.51\ \mu m \quad (9)$$

Actually, the power spectrum of our laser source does not show a Gaussian profile. As such, the PSF is experimentally determined by fitting a Lorentzian function to the measured PSF profile (A-scan) when using a gold mirror sample (Fig 6). For our system we obtained an axial resolution of 8.1 μm, in the air, which corresponds to 6.2 μm in tissue.

B. Sensitivity

Sensitivity is related with the smallest sample reflectivity, $R_{s,min}$, that can be detected, defined as the signal level when SNR=1. In dB units:

$$S_{dB} = 10log_{10}\frac{R_s}{R_{s,min}} \quad (10)$$

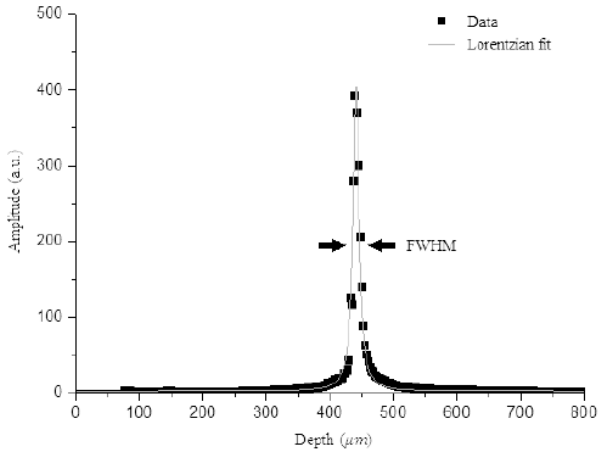

Fig. 6 – Experimental axial resolution measurement using curve fitting to the gold mirror PSF

One way of experimentally measure S is to use a gold mirror (R_s=1) on the sample side. Thus, (6) becomes:

$$S_{dB} = 10log_{10}\frac{1}{R_{s,min}} \quad (11)$$

In terms of the measured quantities, sensitivity of the system can be estimated from the ratio between the output from the optimal reflector (the system point spread function, PSF) and that from the noise (no sample), the latter being defined as the standard deviation of the readings, leading to:

$$S_{dB} = 20log_{10}\frac{PSF_{peak}}{\sigma_{noise}} \quad (12)$$

Notice that the factor 2 arises from the square correlation between the photodetector current and the reflectance, R, that is: $PSF \propto I_D(z) \propto \sqrt{R}$.

One way to experimentally determine the sensitivity is to place a neutral density filter of a known optical density (OD) before the gold mirror. Light will then be doubly attenuated by the filter, resulting in a total attenuation of 20×OD (dB). Added to (12) results in:

$$S_{dB} = 20log_{10}\frac{PSF'_{peak}}{\sigma_{noise}} + 20\times OD \quad (13)$$

In these conditions, a sensitivity of 105 dB was experimentally determined, allowing to calculate $R_{s,min}$ from (11).

C. Dynamic Range

Dynamic range (DR) regards the ratio between the maximum and the minimum reflectivity signal that can be measured within the same A-scan. In OCT, the smallest reflectivity is taken as the standard deviation of the noise floor when we measure the PSF using a gold coated mirror as sample. This way the expression is similar to (8) but all measurements refer to the same A-Scan:

$$S_{dB} = 20log_{10}\frac{PSF_{peak}}{\sigma_{noise}} \quad (14)$$

Experimentally we measured the Dynamic Range always above 55 dB, a value better than the minimum acceptable for biomedical tissues (40-50). Better results were obtained with the inclusion of an electronic 100 MHz low-pass filter at the output of the balanced amplifier to remove high frequency noise. Although the presence of the filter limits the maximum measurement depth, this is not a problem for the experimental setup as the mirror position is far from the filter's influence.

In the case depicted in Fig 7 for the current setup we obtained:

$$D = 20\log\left(\frac{1627.9}{1.1820}\right) = 62.78dB \quad (15)$$

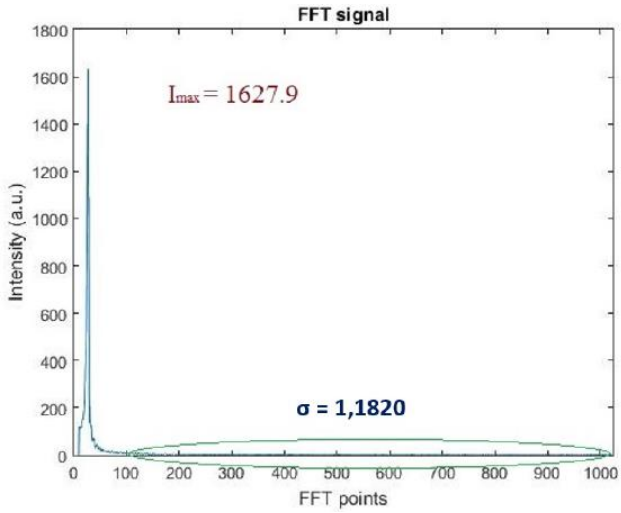

Fig. 7 - Ratio of maximum to the minimum reflectivity that can be measured simultaneously (same A-scan).

D. Sensitivity Roll-off

In OCT, a depth dependent sensitivity fall-off occurs independently of absorption or scattering from the sample. This fall-off, which places a limit to the maximum tissue depth that can be assessed, is primarily due to the washout of spectral fringes caused by the limited spectral sampling resolution of the spectrometer (in case of SD-OCT) or by the limited sweeping resolution and detector bandwidth (in case of SS-OCT). The sensitivity roll-off of our system was evaluated by doing the sensitivity measurement procedure for different axial positions of the mirror, used as sample. The sensitivity roll-off with depth was assessed over an axial range of 4 mm to find it to be less than 1 dB/mm in the first 2.8 mm and about 3 dB/mm thereafter as shown in Fig 8.

V. Conclusions

The presented layout and setup allowed to achieve the required performance for biomedical field and opens the possibility to future developments in the instrumentation and application sides.

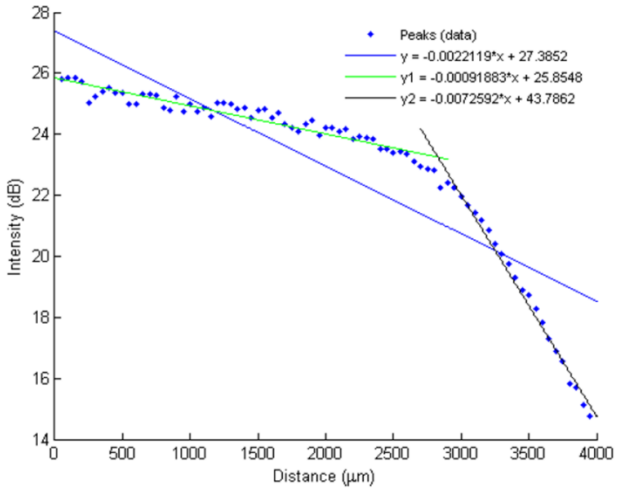

Fig. 8 – Sensitivity measurement over 4 mm depth range. The corner for a depth near 2.8 mm is due to the 100 MHz LP electronic filter. Higher electronic frequencies on the detector signal correspond to higher penetration depths.

Acknowledgment

This study was supported by The Portuguese Foundation for Science and Technology (PEst-UID/NEU/04539/2013) and by FEDER-COMPETE (POCI-01-0145- FEDER-007440).

References

[1] Tomlins P H and Wang R K (2005) Theory, developments and applications of optical coherence tomography. Journal of Physics: Appl. Phys. 38, pp. 2519-2535 DOI 10.1088/0022-3727/38/15/002

[2] Targowski, P Wojtkowski M et al (2004) Complex spectral OCT in human eye imaging in vivo. Optics Communications 229 pp. 79-84.

[3] Marschall S, Sander B et al (2011) Optical coherence tomography – current technology and applications in clinical and biomedical research. Anal Bioanal Chem 400 pp. 2699-2720 DOI 10.1007/s00216-011-5008-1

[4] Huang D, Swanson C et al (1991) Optical Coherence Tomography. Science, 254(5035) pp. 1178-1181

[5] Silva, S., Domingues, J., Agnelo J, Morgado A, Bernardes R (2014), Development of an Optical Coherence Tomograph for Small Animal Retinal Imaging, IFMBE Proceedings Volume 41, , pp 419-422. DOI: 10.1007/978-3-319-00846-2_104

[6] W. Wieser, B. R. Biedermann, T. Klein, C. M. Eigenwillig, and R. Huber, "Multi-megahertz OCT: High quality 3D imaging at 20 million A-scans and 4.5 GVoxels per second.," Opt. Express, vol. 18, no. 14, pp. 14685–14704, 2010.

[7] M. D Bayleyegn, H. Makhlouf et al (2012) Ultrahigh Resolution spectral-domain optical coherence tomography at 1.3 μm using a broadband superluminescent diode light source, Opt Commun., vol 285, nº 24, pp 5564-5569